EPJ Web of Conferences **105**, 01001 (2015)
DOI: 10.1051/epjconf/201510501001

Recent results from the AMS-02 experiment

Manuela Vecchi[a] on behalf of the AMS-02 Collaboration

Instituto de Física de São Carlos, Universidade de São Paulo, CP 369, 13560-970, São Carlos, SP, Brazil

Abstract. The AMS-02 detector is a large acceptance magnetic spectrometer operating onboard the International Space Station since May 2011. The main goals of the detector are the search for antimatter and dark matter in space, as well as the measurement of cosmic ray composition and flux. Precise measurements of cosmic ray positrons and electrons are presented in this document, based on 41×10^9 events collected during the first 30 months of operations.

1. Introduction and detector layout

The Alpha Magnetic Spectrometer is a general purpose particle physics detector, operating in space since May 2011. It will achieve a unique long duration mission, aiming at performing antimatter and dark matter searches, as well as cosmic ray composition and flux measurements. The experiment is installed onboard the International Space Station (ISS), that follows a Low Earth Orbit at about 400 km altitude with respect to the Earth surface, well located to detect cosmic particles before they interact with the outer layers of the atmosphere. This makes the ISS one the most interesting environments to perform cosmic rays studies. AMS being a space-born detector, the data acquisition parameters change as a function of the detector position with respect to Earth, as it is shown in Fig. 1. The measurements presented in this document are based on the data collected during the first 30 months of operations of the detector, from May 19th 2011 to November 26th 2013. The detector is composed of several sub-detectors, as shown in Fig. 2. In this period 41×10^9 cosmic ray events were detected. The silicon tracker [1] measures the trajectory and absolute charge $|Z|$ of cosmic rays by performing multiple measurements of the coordinates and energy loss. Together with the 0.14 T permanent magnet, the tracker measures the particle rigidity $R = pc/Ze$, where p is the momentum. The Transition Radiation Detector (TRD) [2] identifies the particle as an electron/positron. The four layers of the Time of Flight (TOF) [3] measure the particles charge and ensure that the particle is downward-going. The high efficiency (∼99.999%) anti-coincidence counters [4] inside the magnet bore are used to reject particles outside the geometric acceptance. The Ring Imaging CHerenkov detector (RICH) [5] measures the particles charge and velocity. The imaging Electromagnetic Calorimeter (ECAL) [6] identifies the particle as an electron/positron and measures its energy.

The AMS-02 detector has been extensively calibrated using a test beam at CERN with e^- and e^+ from 10 to 290 GeV, with protons at 180 and 400 GeV, and with $\pi^\pm$ from 10 to 180 GeV.

1.1. Lepton-hadron separation

Electrons and positrons only account for a tiny fraction of the cosmic rays: e^- are $\sim10^{-2}$ less abundant than protons, while e^+ are $\sim10^{-4}$ less abundant than protons. However, the measurement of their fluxes can provide important informations to understand the nearby universe, as their detection horizon is limited to few kiloparsecs, due to energy losses. Three main sub-detectors provide clean and redundant identification of positrons and electrons with independent suppression of the proton background. These are the TRD (above the magnet), the ECAL (below the magnet) and the tracker. The matching of the ECAL energy and the momentum measured with the tracker (*E/p* in the following) greatly improves the proton rejection. To differentiate between $e^\pm$ and protons in the TRD, a TRD estimator formed by the ratio of the log-likelihood probability of the $e^\pm$ hypothesis to that of the proton hypothesis in each layer is used. The proton rejection power of the TRD estimator at 90% $e^\pm$ efficiency is 10^3 to 10^4 [7], as estimated using flight data. To cleanly identify electrons and positrons in the ECAL, a Boosted Decision Tree [8] estimator is build using the 3D shower shape. The ECAL proton rejection power reaches 10^4 when combined with the *E/p* matching requirement.

2. The positron fraction measurement

The positron fraction (PF) is defined as the ratio between the positron flux and the electron plus positron flux, i.e. $\frac{\Phi_{e+}}{(\Phi_{e^+}+\Phi_{e^-})}$. As the acceptance and efficiencies simplify in the ratio, the positron fraction is given by the ratio of the number of events. Events are selected by requiring a track in the TRD and in the tracker, a shower in the ECAL, and a measured velocity $\beta \sim 1$ in the TOF consistent with a downward-going particle with charge one. To reject secondary positrons and electrons produced by the interaction of primary cosmic rays with the atmosphere,

[a] e-mail: manuela.vecchi@ifsc.usp.br

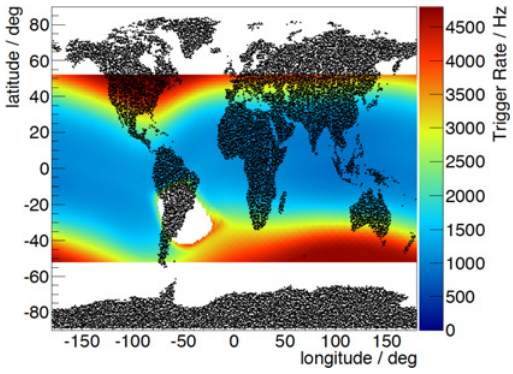

Figure 1. Trigger rate as a function of orbital position. Variations are correlated with the geomagnetic cutoff rigidity.

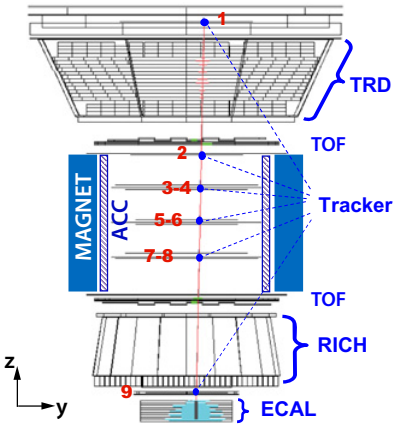

Figure 2. A 369 GeV positron event as measured by the AMS detector on the ISS, in the (y-z) plane.

the energy measured with the ECAL is required to exceed, by a factor of 1.2, the maximum Størmer cutoff [10] for either a positron or electron at the geomagnetic location where the particle was detected and at any angle within the acceptance. In each energy bin, the two-dimensional reference spectra for $e^{\pm}$ and the background are fit to data in the TRD estimator-log(E/p) plane. The template fit is used to estimate the number of electrons plus positrons reconstructed with a positive charge sign, N_+, and the number of electrons plus positrons reconstructed with a negative charge sign, N_-. A maximum-likelihood fit yields N_+, N_-, and the number of protons in the bin. Finally, these numbers are corrected for charge confusion (CC), i.e. the fraction of electrons misidentified as positrons. Charge confusion has two main sources: the finite resolution of the tracker as well as multiple scattering, and the production of secondary particles and radiation along the track of the primary particle in the tracker. Both sources are found to be well reproduced by the Monte Carlo. CC is mitigated by a cut on the E/p matching and additional cuts on the tracker track quality, the charge measured in the tracker and in the TOF. The CC reference spectra are derived from the Monte Carlo simulation.

The PF from 0.5 GeV to 500 GeV is shown in Fig. 3. It is steadily increasing above 10 GeV, up to about 250 GeV: above this energy it is found to be no longer dependent on energy. The rise in the PF is in contrast with the

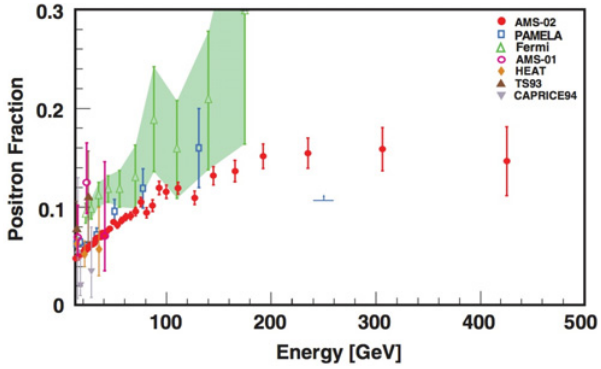

Figure 3. The positron fraction as a function of energy [9]: AMS-02 data (red dots) from 0.5 to 500 GeV are compared to previous experiments. The horizontal linear scale emphasizes the precision of AMS-02 data with respect to previous measurements, as well as the extended energy range.

hypothesis that positrons are only secondary particles [11–13]. Given our current understanding of the cosmic rays propagation in the Galaxy, positrons are produced in standard astrophysical processes, such as the spallation of primary cosmic rays into the interstellar medium. The PF measurement implies the need for a primary component of positrons, namely the existence of a source of positrons in the vicinity of the Solar System. Positron-electron pairs could be produced and accelerated by nearby rapidly rotating neutron stars, i.e. pulsars [14, 15]. Besides standard astrophysical mechanisms, exotic scenarios like the annihilation of dark matter (DM) particles in the Milky Way halo could also be probed. Positrons constitute a good channel to search for DM, given their low abundance in cosmic radiation [16–19]. On top of the antiparticles from standard astrophysical processes, the messengers of DM annihilation would generate distortions in the measured fluxes.

The PF has been fit to a minimal model with 7 parameters. In this model the positron flux is described by a power law term, with spectral index γ_{e^+}, indicating the secondary production from standard astrophysical processes, and a charge-symmetric source term with a power law and an exponential cutoff E_S:

$$\Phi_{e^+} = C_{e^+} E^{-\gamma_{e^+}} + C_S E^{-\gamma_S} e^{-E/E_S}. \quad (1)$$

The electron flux is also parametrised using a power law, with different normalisation and spectral index with respect to positrons, since e^- are thought to be also primaries, produced in galactic sources such as SuperNova Remnants. The charge-symmetric source term is also added to the parametrisation of the electron flux:

$$\Phi_{e^-} = C_{e^-} E^{-\gamma_{e^-}} + C_S E^{-\gamma_S} e^{-E/E_S}. \quad (2)$$

A fit of this model to the data with their total errors in the energy range from 1 to 500 GeV yields a $\chi^2/ndof = 36.4/58$ and $1/E_S = 1.84 \pm 0.58$ TeV^{-1} [9]. The AMS-02 measurement, together with the fit are shown in Fig. 4. No fine structures are observed in the data. The same

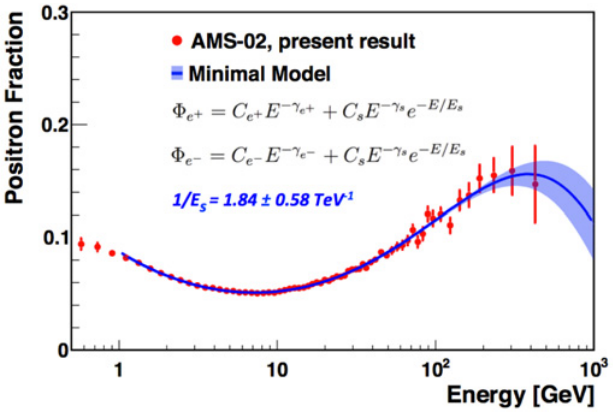

Figure 4. The positron fraction measured by AMS-02 [9] and the fit of a minimal model (solid curve, see text) and the 68% C.L. range of the fit parameters (shaded). For this fit, both the data and the model are integrated over the bin width. The error bars are the quadratic sum of the statistical and systematic uncertainties.

model with no exponential cutoff, i.e. with $1/E_S$ set to 0, is excluded at the 99.9% C.L.

Several papers report dedicated analysis on the interpretation of AMS-02 electron and positron measurements in terms of astrophysical or exotic origin (see for example [20], [21] and [22]). It is possible to show that if the positron excess is due to the annihilation of DM in the vicinity of the Solar System, the mass of the DM particle has to be higher than 500 GeV. Moreover, the direct annihilation into lepton pairs seems disfavoured, while direct annihilation into quarks, Z, W, or Higgs boson pairs is reproducing well the data, with best-fit masses between 10 and 40 TeV. The interpretation of the PF rise in terms of pulsars is also viable: few pulsars in the vicinity of the Solar system have been identified as possible candidates to satisfy the experimental measurements.

3. The positron and electron flux measurement

The measurement of the separate fluxes of electrons and positrons is needed for a deeper understanding of the PF measurement, as in principle the observed rise in the PF could either be due to an excess of positrons or to a loss of electrons. The isotropic flux of cosmic rays electrons and positrons in each energy bin E, of width ΔE, is given by [23]:

$$\Phi(E) = \frac{N_e(E)}{A_{eff} \cdot T(E) \cdot \Delta(E)} \qquad (3)$$

where $N_e(E)$ is the number of electrons or positrons with energy between E and $E + \Delta E$, A_{eff} is the effective acceptance, $T(E)$ is the exposure time. The effective acceptance A_{eff} is the product of the detector geometric acceptance ($\sim$500 cm^{2}sr) and the selection efficiency, estimated with simulated events and validated with a pure sample of electron events identified in the data. The trigger efficiency is 100% above few GeV, and it is estimated using minimum bias triggered events. The exposure time is evaluated as a function of energy and it takes into account the lifetime of the experiment which depends on its orbit location and on the geomagnetic cutoff. To identify downward-going particles of charge one, cuts are applied on the velocity measured by the TOF and on the charge reconstructed by the tracker, the upper TOF planes, and the TRD. To reject positrons and electrons produced by the interaction of primary cosmic rays with the atmosphere, the minimum energy within the bin is required to exceed 1.2 times the geomagnetic cutoff. Over a sample of well reconstructed particles with one shower in the ECAL and one track in the TRD and in the tracker, the identification of signal events is performed applying an additional cut on E/p, followed by a fixed cut in the ECAL estimator to further reduce the proton background. The number of signal and background event is estimated for each energy bin performing a template fit procedure, similar to the one described in section 2. In total, 9.23×10^6 events are identified as electrons and 0.58×10^6 as positrons.

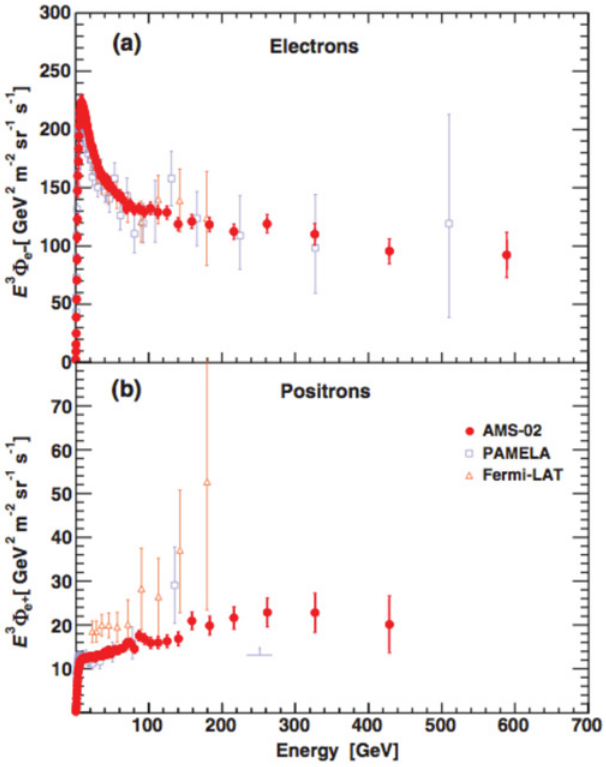

Figure 5. AMS-02 electron (top) and positron (bottom) fluxes [23], rescaled by the cube of the energy, as a function of energy. AMS-02 data are shown in red, compared to previous measurements.

The energy resolution of the ECAL is below 2% at energies higher than 80 GeV [6] and the absolute energy scale is verified by using minimum ionising particles and the ratio between the energy, measured by the ECAL, and the momentum, measured by the tracker. These results are compared with the Test Beam values where the beam energy is known to high precision. Between 10 and 290 GeV (Test Beam energies), the uncertainty on the absolute scale is $\sim$2%, while it is 4% up to 700 GeV. The statistical error dominates above 50 GeV in the measurement of positrons, while the systematic and statistical errors are comparable for electrons, above 200 GeV (see Table 1 in [23]). Figure 5 shows the

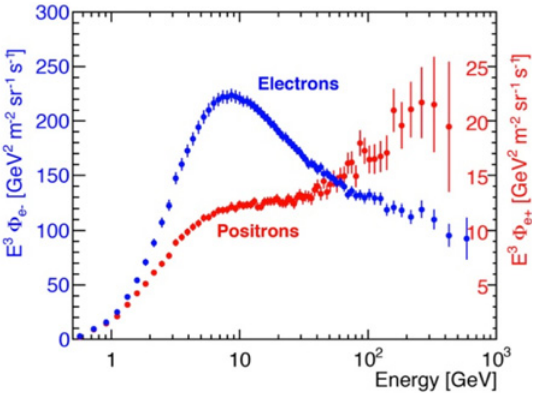

Figure 6. AMS-02 positron and electron fluxes [23], rescaled by the cube of the energy.

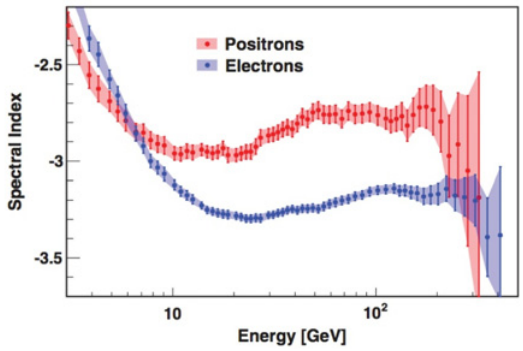

Figure 7. Spectral index for electrons (in blue) and positrons (in red), as a function of energy [23].

electron (top) and positron (bottom) fluxes as a function of energy, multiplied by the cube of the energy, compared to previous measurements. The electron flux is shown from 0.5 GeV up to 700 GeV, while the positron flux is shown from 0.5 GeV up to 500 GeV. The horizontal linear scale highlights the precision and good quality of AMS-02 data compared with previous measurements. Figure 6 shows the electron and positron fluxes compared. The electron and positron fluxes are different in magnitude and in their energy dependence. Figure 7 shows the spectral index of electrons (in blue) and positrons (in red), as a function of energy: we can see that neither the positron nor the electron flux can be described by a single power law. Above 20 GeV, positron flux is significantly harder than the electron flux, implying that the observed rise in the PF is actually due to an excess of positrons and not to a loss of electrons. This indicates that high energy positrons have a different origin from that of electrons. A better understanding of these phenomena can be achieved by continuing to collect data up to the TeV region and by measuring other important channels, such as the antiproton to proton ratio.

Figure 8 shows the AMS-02 combined electrons plus positrons flux, rescaled by the cube of the energy, as a function of energy, together with previous measurements. A major experimental advantage of the combined lepton flux analysis compared to the measurement of the individual positron and electron fluxes, particularly at high energies, is that the event selection does not depend on the

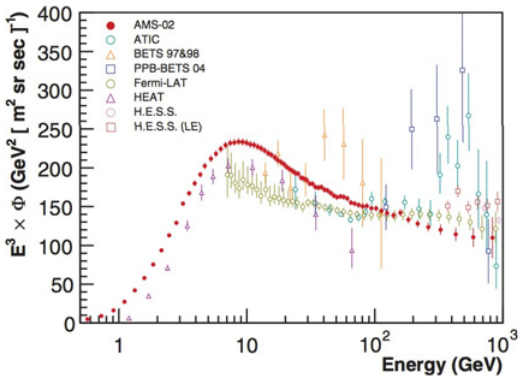

Figure 8. AMS-02 combined positrons plus electrons flux, rescaled by the cube of energy, as a function of energy [24], together with the most recent measurements from other experiments. See [24] for the complete list of references.

sign of the charge, implying higher selection efficiency. Consequently, this measurement is extended to 1 TeV with less overall uncertainty over the entire energy range. Given the high statistics and high precision of the measurement, the spectral index of the combined flux has also been measured and, for energies higher than 30 GeV, it is found to be compatible with a single power law.

4. Conclusions

The AMS-02 detector is operating aboard the International Space Station since May 2011. The main goals of the experiment are the precise measurements of the cosmic ray fluxes in the GeV to TeV range, as well as the search for primordial antimatter and dark matter. In this document we present the positron fraction measurement, as well as the electron and positron fluxes. These measurements are performed with increased precision with respect to previous measurements, and a previously unexplored energy region has been studied. The results show that the observed rise in the positron fraction is due to a hardening of the positron flux and not to a loss of electrons. Moreover, the electron and positron fluxes are different in magnitude and energy dependence, implying that different phenomena are involved in their production. Given the long duration of the mission and the good quality of AMS data, a better understanding of these phenomena will be achieved by collecting data up to the TeV region, and by studying other important channels such as antiprotons, protons and heavier nuclei.

The author is grateful to São Paulo Research Foundation (FAPESP) for the financial support (grant #2014/19149-7 and #2014/50747-8). The author is thankful to Simona Toscano and Elisa Prandini for the kind invitation to the SuGar workshop.

References

[1] B. Alpat et al., Nucl. Instrum. Meth. A **613**, 207 (2009)
[2] T. Kirn et al., Nucl. Instrum. Meth. A **706** (2013) 43–47
[3] V. Bindi et al., Nucl. Instr. Meth. A **743** (2014) 22–29
[4] Ph. von Doetinchem et al., Nucl. Phys. Proc. Suppl. **197** (2009) 15–18

[5] M. Aguilar-Benitez et al., Nucl. Instr. Meth. A **614** (2010) 237–249
[6] C. Adloff et al., Nucl. Instr. Meth. A **714** (2013) 147–154
[7] L. Accardo et al., Phys. Rev. Lett. **110**, 141102 (2013)
[8] Roe, Byron P. et al., Nucl. Instr. Meth. A **543** (2005) 2–3, 577–584
[9] M. Aguilar et al., Phys. Rev. Lett. **113**, 121101 (2014)
[10] C. Stormer. 1950. The Polar Aurora (Oxford University Press, London)
[11] T. Delahaye et al., Astr. Astroph. **501**, 821–833 (2009)
[12] I. V. Moskalenko et al., Astroph. J. **493**, 694–707 (1998)
[13] L. Maccione et al., Phys. Rev. Lett. D **89**, 083007 (2014)
[14] D. Hooper et al., JCAP 0901 (2009) 025
[15] T. Linder and S. Profumo, Astroph. J. **772** (2013) 18
[16] S. Profumo et al., JCAP **0407** (2004)
[17] D. Hooper et al., Phys. Rev. D **171** (2005)
[18] E. Ponton et al., JHEP **0904** (2009) 080
[19] L. Bergstrom et al., Phys. Rev. Lett. **103**, 031103 (2009)
[20] M. Di Mauro et al., JCAP 04 (2014) 006
[21] M. Boudaud et al., Astr. Astroph. **575**, A67 (2015)
[22] Q. Yuan and X.B. Bi, JCAP **1503** (2015) 033
[23] M. Aguilar et al., Phys. Rev. Lett. **113**, 121102 (2014)
[24] M. Aguilar et al., Phys. Rev. Lett. **113**, 221102 (2014)